Supplementary information

Facile engineering of interactive double network hydrogels for heart valve regeneration

Jinsheng Li[1,2]#, Weihua Qiao[1]#, Yuqi Liu[1], Huiling Lei[2], Shuangshuang Wang[3], Yin Xu[1], Ying Zhou[1], Shuyu Wen[1], Zhuoran Yang[2], Wenyi Wan[1], Jiawei Shi[1], Nianguo Dong[1]*, Yuzhou Wu[2]**

1. Department of Cardiovascular Surgery, Union Hospital, Tongji Medical College, Huazhong University of Science and Technology, 1277 Jiefang Avenue, Wuhan 430022, China.
2. Hubei Engineering Research Center for Biomaterials and Medical Protective Materials, Hubei Key Laboratory of Bioinorganic Chemistry & Materia Medica, State Key Laboratory of Materials Processing and Die & Mould Technology, School of Chemistry and Chemical Engineering, Huazhong University of Science and Technology (HUST), 1037 Luoyu Road, Wuhan 430074, China.
3. School of Life Science and Chemistry, Wuhan Donghu University, Wuhan 430212 P.R. China.

# These authors contributed equally to this work.

*Correspondence to: Yuzhou Wu, Hubei Engineering Research Center for Biomaterials and Medical Protective Materials, Hubei Key Laboratory of Bioinorganic Chemistry & Materia Medica, State Key Laboratory of Materials Processing and Die & Mould Technology, School of Chemistry and Chemical Engineering, Huazhong University of Science and Technology (HUST), 1037 Luoyu Road, Wuhan 430074, China, Email: wuyuzhou@hust.edu.cn.

Nianguo Dong, Department of Cardiovascular Surgery, Union Hospital, Tongji Medical College, Huazhong University of Science and Technology, 1277 Jiefang Avenue, Wuhan 430022, China, Email: dongnianguo@hotmail.com.

Jiawei Shi, Department of Cardiovascular Surgery, Union Hospital, Tongji Medical College, Huazhong University of Science and Technology, 1277 Jiefang Avenue, Wuhan 430022, China, Email: shijiawei@hotmail.com.

Catalogue

Supplementary Methods

Detection of H_2S release from DETU and MECT by WSP-1 probe

Washington State Probe-1 (WSP-1, 5 mM) stock solution was prepared in dimethyl sulfoxide (DMSO). DETU (16 mM), MECT (16 mM) and cysteine (32 mM) stock solutions were prepared in ultrapure water. Then, 0.5 mL of DETU and MECT stock solution was mixed with 0.5 mL of cysteine stock solution and 2 μL WSP-1 stock solution, respectively. And the fluorescence intensity was detected at different time points with an microplate reader (Varioskan LUX, Thermo Fisher Scientific, USA, Ex/Em=465/515 nm).

Preparation of PEG/PSBMA double-network hydrogel

TCDI (90 mg/mL) stock solution was prepared in N'N'-dimethylformamide (DMF). 4-arm-PEG-NH_2 (0.4 g/mL), sulfobetaine methacrylate (SBMA, 2.4 g/mL), N'N'-Methylenebisacrylamide (MBA, 3 mg/mL) and azodiisobulimidazoline hydrochloride (AIBA, 60 mg/mL) stock solutions were prepared in ultrapure water.The PEG/PSBMA double network hydrogel is prepared by a one-step method. In brief, 50 μL 4-arm-PEG-NH_2 stock solutions, 50 μL SBMA stock solutions, 10 μL TCDI stock solutions, 10 μL MBA stock solutions and 10 μL AIBA stock solutions were added to 70 μL ultrapure water. The mixed solution was shaken and mixed uniformly, and reacted at 37 ℃ for 24 h to form a hydrogel. Pure PSBMA hydrogels are also prepared with the same procedure without adding 4-arm-PEG-NH_2 and TCDI.

Sample morphology and composition analyses

DHV, GV, T-DHV, PEG-DHV, PEG/PSBMA-DHV were frozen in liquid nitrogen and subsequently removing the remaining water using a freeze dryer. The morphology of samples was analyzed using scanning electron microscopy (SEM; GeminiSEM300, Carl Zeiss, Germany) at an accelerating voltage of 5 kV after surface gold spraying. The surface element distribution of the samples was analyzed using energy dispersive spectroscopy (EDS; Hitachi, Japan), and elemental analysis (EA; EA3000, Euro Vector, Italy). The surface functional groups and chemical bonds of the samples were investigated using an attenuated total reflection Fourier-transform infrared (ATR-FTIR) spectrophotometer (Nicolet iS50R, Thermo Fisher

Scientific, USA) with a wavenumber range of 500-3000 cm^{-1} and a resolution of 4 cm^{-1}. A contact angle analyzer (Kruss, USA) was used to measure the hydrophilicity of the samples.

Evaluation of H_2S release ability and immunomodulatory capacity of 4-arm-PEG-NH_2 and SBMA

In order to further exclude the influence of 4-arm-PEG-NH_2 and SBMA on H_2S release ability, 10 wt.% 4-arm-PEG-NH_2 and 20 wt.% SBMA were dissolved in Dulbecco's Modified Eagle Medium (DMEM, high glucose, Hyclone, USA) supplemented with 10% FBS (Gibco, USA), 100 unit/mL penicillin and 100 μg/ml streptomycin (Biosharp, China) respectively, which was further used to evaluate the H_2S release capacity by the detection paper as previously reported.[1] Briefly, the filter paper strips were soaked in 20 mM lead acetate solution for 10 min and then placed in the oven to dry. Then, the filter paper strip was placed above the 10 wt.% 4-arm-PEG-NH_2 and 20 wt.% SBMA solution in a closed container (microcentrifuge tube) and incubated at 37 °C. When H_2S is produced, the filter paper will turn black. At the same time, in order to further exclude the influence of 4-arm-PEG-NH_2 and SBMA on immunoregulatory capacity, Raw264.7 was incubated for 48 h with complete medium containing 10 wt.% 4-arm-PEG-NH_2 and 20 wt.% SBMA respectively, and the proportion of CD206+ macrophages was analyzed by flow cytometry.

Evaluation of immunomodulatory capacity of 4-arm-PEG-NH_2, SBMA, DHV, GV, T-DHV, PEG-DHV and PEG/PSBMA-DHV in the presence of cysteine

To compare the immunomodulatory capacity of T-DHV, PEG-DHV, and PEG/PSBMA-DHV in the presence or absence of cysteine. RAW264.7 was digested, counted, and cultured in 12-well plates at the density of 170,000 cells/well overnight. The DHV samples were treated similar as for cytotoxicity assay and subsequently added to the macrophages to co-culture for 48 h with or without 0.8 M cysteine. And then, M2 macrophages were labeled with FITC-anti mouse CD206 (Abcam, UK) according to the supplier's instructions, and the proportion of M2 macrophage was quantified by flow cytometry (CytoFLEX, BD Biosciences, Oxford, UK).

The effect of paracrine products of macrophage on HUVECs and BMSCs behavior

Collection of conditional medium (CM). RAW264.7 was digested, counted, and cultured in 12-well plates at the density of 170,000 cells/well overnight, which were further co-cultured

with samples for 48 h. The supernatant in the 12-well plate was collected, and the CM was obtained by centrifugation at 1500 rpm.

In vitro cell migration assay. The cell migration assay was performed as previously reported.[2] In brief, HUVECs were seeded in 24-well plates, and wounds were made with 1 mL sterile pipette tips. Detached cells were washed with PBS buffer and added 50% CM and 50% complete ECM medium. After 24 h incubation, cells were stained with crystal violet dye (Beyotime, China) and cells migrating to the scratched area were photographed under the bright-field microscopy (Zeiss, Germany). The migration rate was calculated:

Migration rate = [(wound length at 0 h - wound length at 24 h) / wound length at 0 h)] × 100%

In vitro BMSCs migration. The 24-well plates and transwell system (8 metric linear unit pore, Corning Life Sciences) was used to assess the vitro migration, as previously reported.[3] Briefly, the 1×10^4 cells/well of BMSCs were seeded in the upper face of the transwell filter. After 4 h, detached cells were washed with PBS buffer, and CM and complete medium with ratio of 1: 1 were added. After 24 h, the transwell filters were removed, washed with PBS and the cells were strained by crystal violet dye solution (Beyotime, China). And then, the upper face of the transwell filters was clean with a cotton swab. The BMSCs in the lower face of filters were imaged under the bright-field microscopy (Zeiss, Germany). The number of transwell cell migration in each image were counted using ImageJ software.

Statistics and reproducibility

Statistical analysis was performed using GraphPad Prism 8.0. Each experiment was repeated independently at least three times and with similar results. All measurements were expressed as mean ± SD, the differences were considered significant at $p < 0.05$ (** $P < 0.01$, *** $P < 0.001$, **** $P < 0.0001$). T-test was used for comparison between the two groups, and one-way ANOVA with Bonferroni-corrected t-test was used for comparison more than two groups. The correlation was analyzed using a Pearson correlation test.

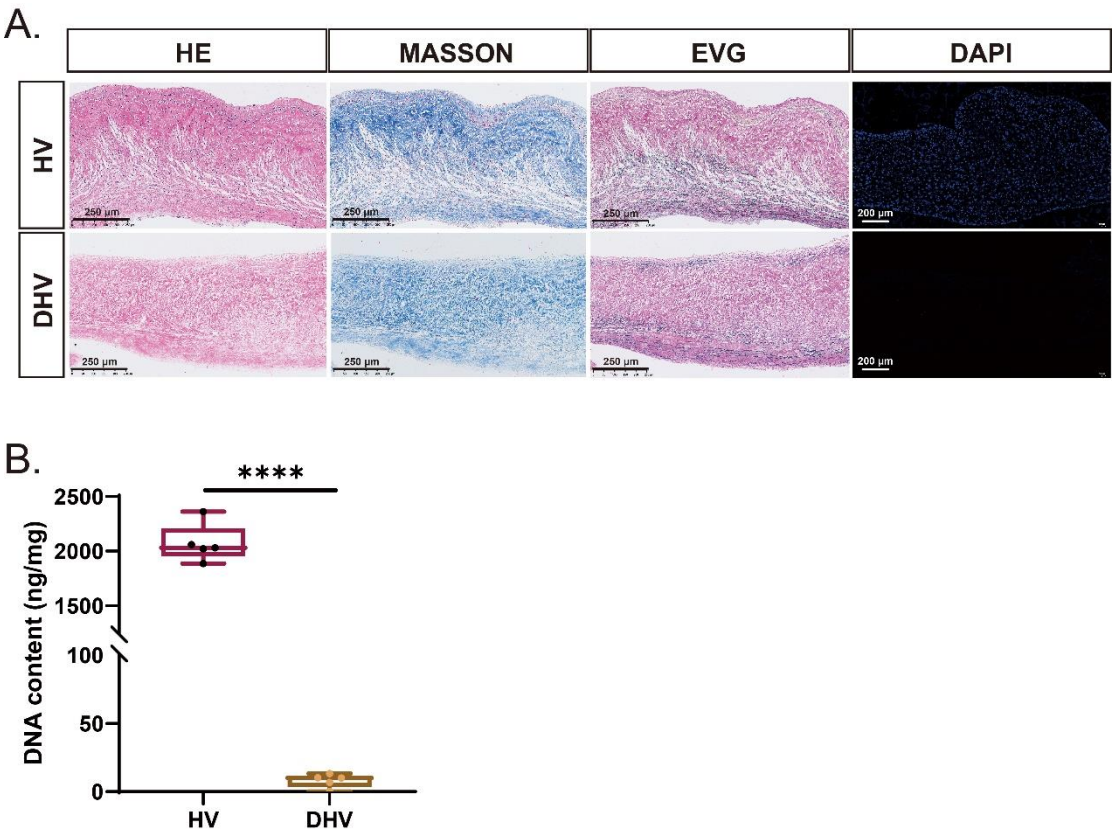

Supplementary Figure. 1 Characterization of the effect of decellularization strategies. A) Before and after decellularization, sections were stained with HE, Masson, EVG and von Kossa. HE for cell and extracellular matrix, Masson stain for collagen, EVG stain for elastin, DAPI (blue) for cell. B) DNA content detection (n=5). Data were expressed as mean ± SD, *P < 0.05, **P < 0.01, ***P < 0.001, and ****P < 0.0001. n means the number of independent experiments. For box plots, the lower edge denotes the first quartile (Q1, or the 25th percentile) of the data, the central line within the box signifies the median (Q2, or the 50th percentile), while the upper edge of the box corresponds to the third quartile (Q3, or the 75th percentile). The lower whisker extends to the minimum value, indicating its range of variation, and the upper whisker reaches the maximum value, demonstrating its variability. T-test was used for analyzing the data.

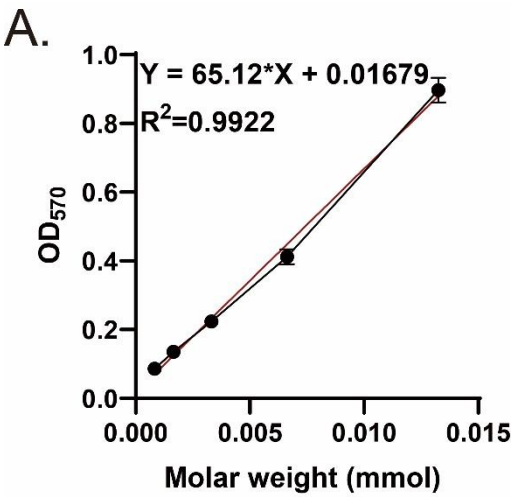

Supplementary Figure. 2 The standard curve of the amino group with ethylenediamine as the standard sample based on ninhydrin method (n=5). n means the number of independent experiments.

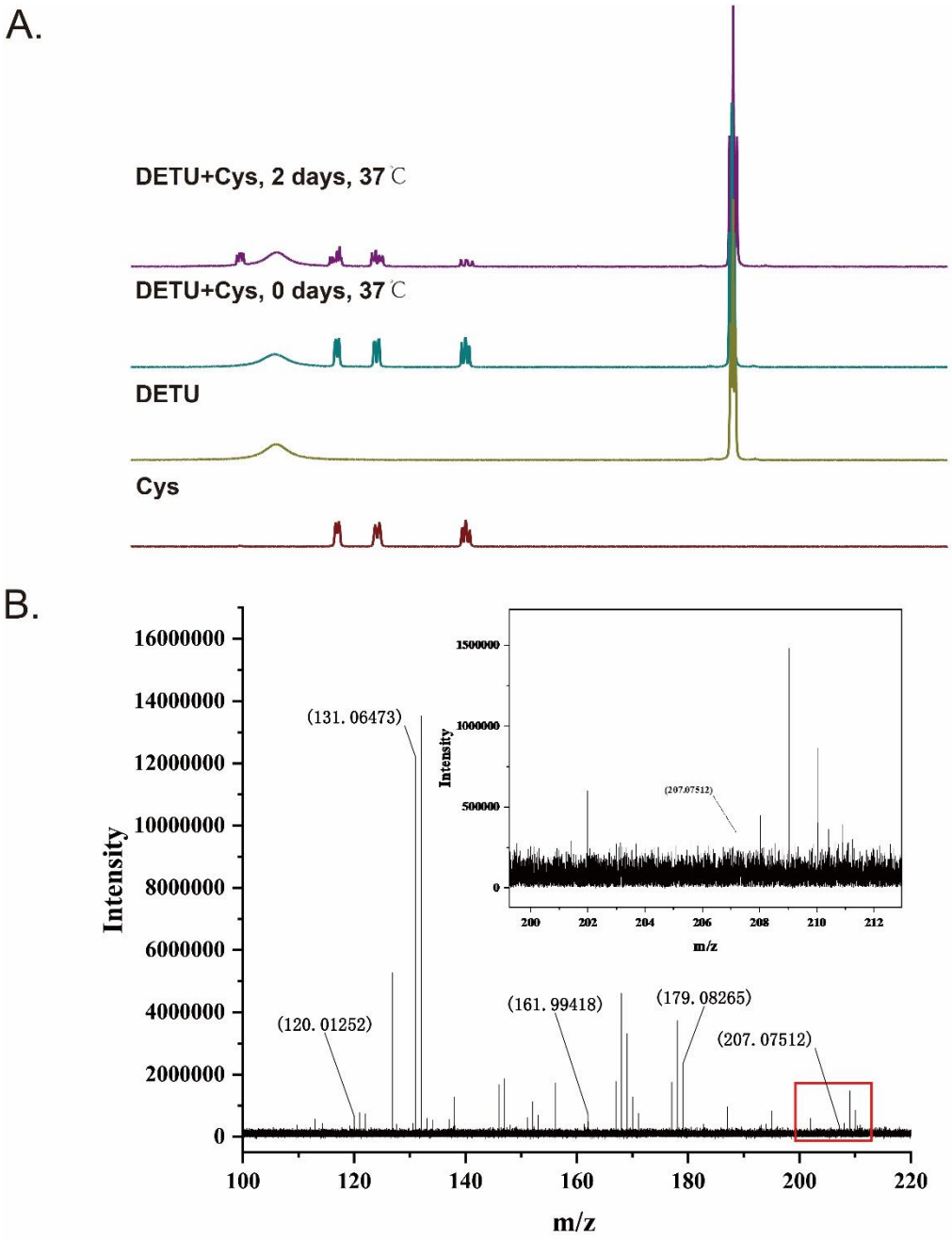

Supplementary Figure. 3 Study on H2S release mechanism of thiourea. A) NMR map of DETU reaction products in the presence of cysteine. DETU was used as a model molecule for thiourea. Cysteine, DETU, DETU+ cysteine (0day) were used as controls for product analysis. B) mass spectrum of DETU reaction products in the presence of cysteine. d, MS:C6H11N2O2S2-,[(M-H)-]: calcd.: 207.03; found: 207.07; e, MS:C4H4NO2S2-,[(M-H)-]: calcd.: 161.97; found: 161.99; f, MS:C4H5NO3S22-,[(M-2H)2-]: calcd.: 178.97; found:179.08.

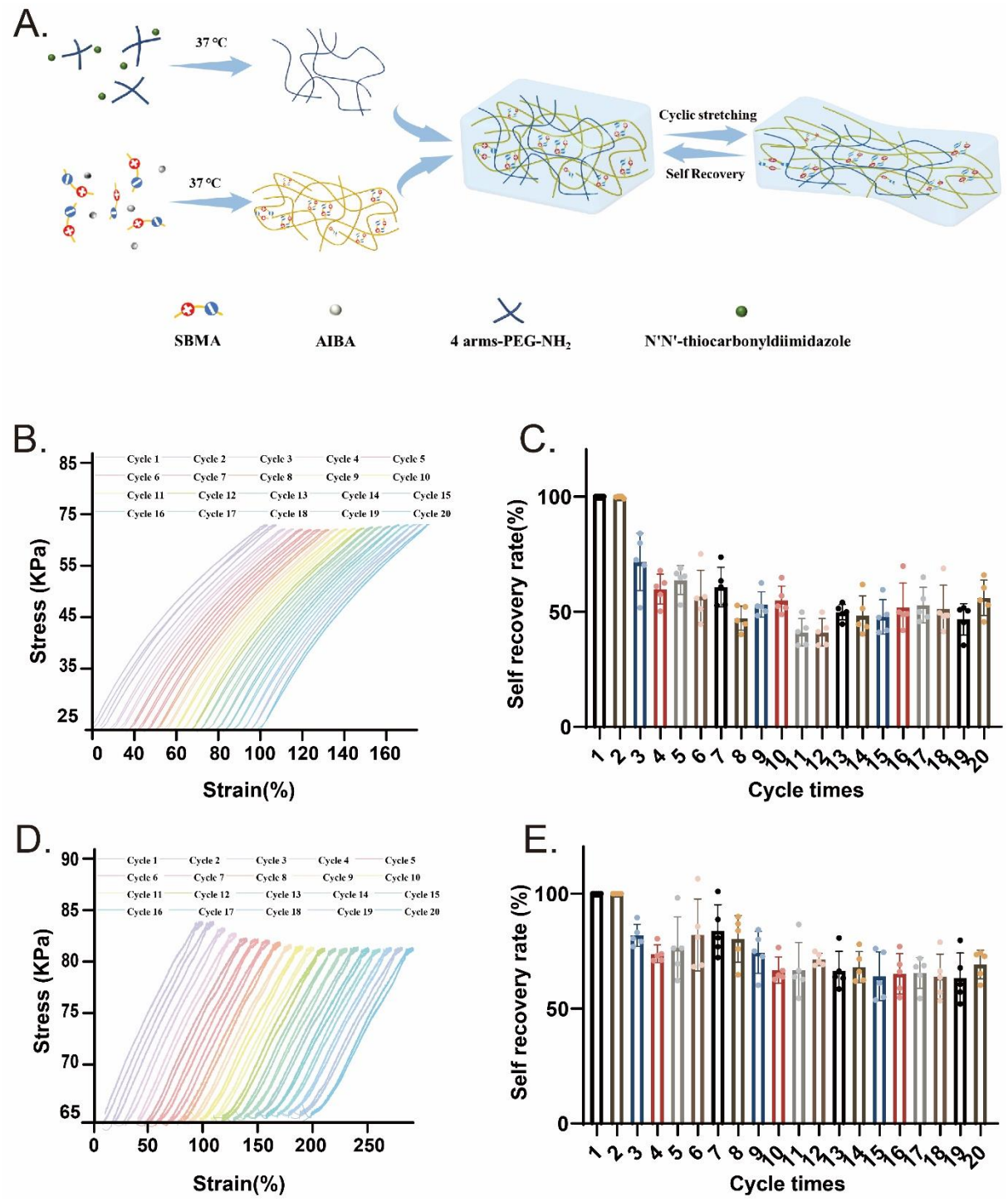

Supplementary Figure. 4 Construction and characterization of PEG/PSBMA dual network hydrogels. A) schematic overview presenting the fabrication process of PEG/PSBMA dual network hydrogel. B) Stress-strain curves of PSBMA hydrogel for each stretching cycle. Strain: 100%, rate: 18 mm/min. C) Self-recovery rate statistics of PSBMA hydrogels (n=5). D) Stress-strain curves of PEG/PSBMA dual network hydrogels for each stretching cycle. Strain: 100%, rate: 18 mm/min. E) Self-recovery rate statistics of PEG/PSBMA dual network hydrogels (n=5).

Data were expressed as mean ± SD, *P < 0.05, **P < 0.01, ***P < 0.001, and ****P < 0.0001. n means the number of independent experiments.

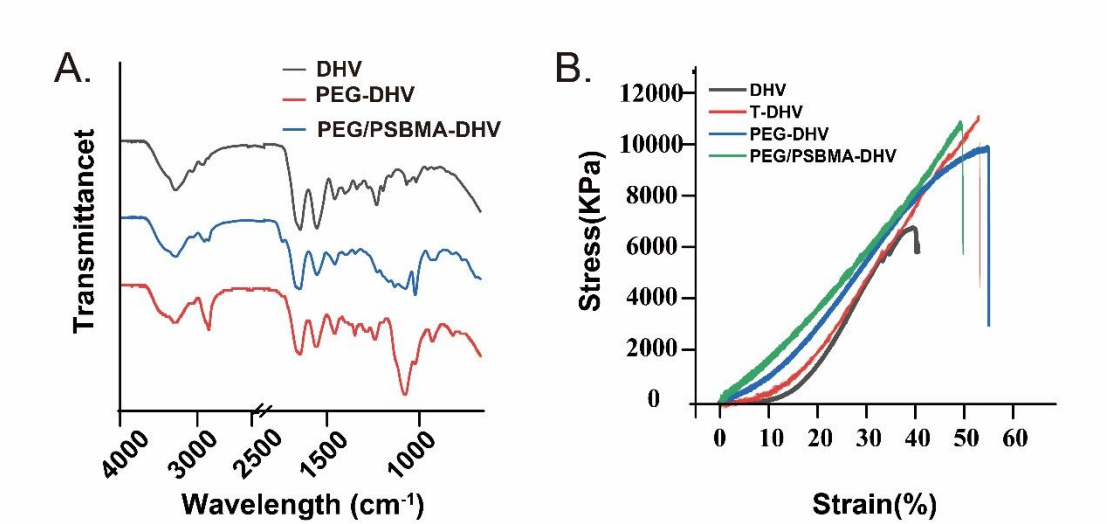

Supplementary Figure. 5 Construction and characterization of PEG/PSBMA-DHV. A) infrared spectroscopy of DHV, PEG-DHV and PEG/PSBMA-DHV. B) Stress-strain curves of DHV, T-DHV, PEG-DHV and PEG/PSBMA-DHV. Rate: 18 mm/min.

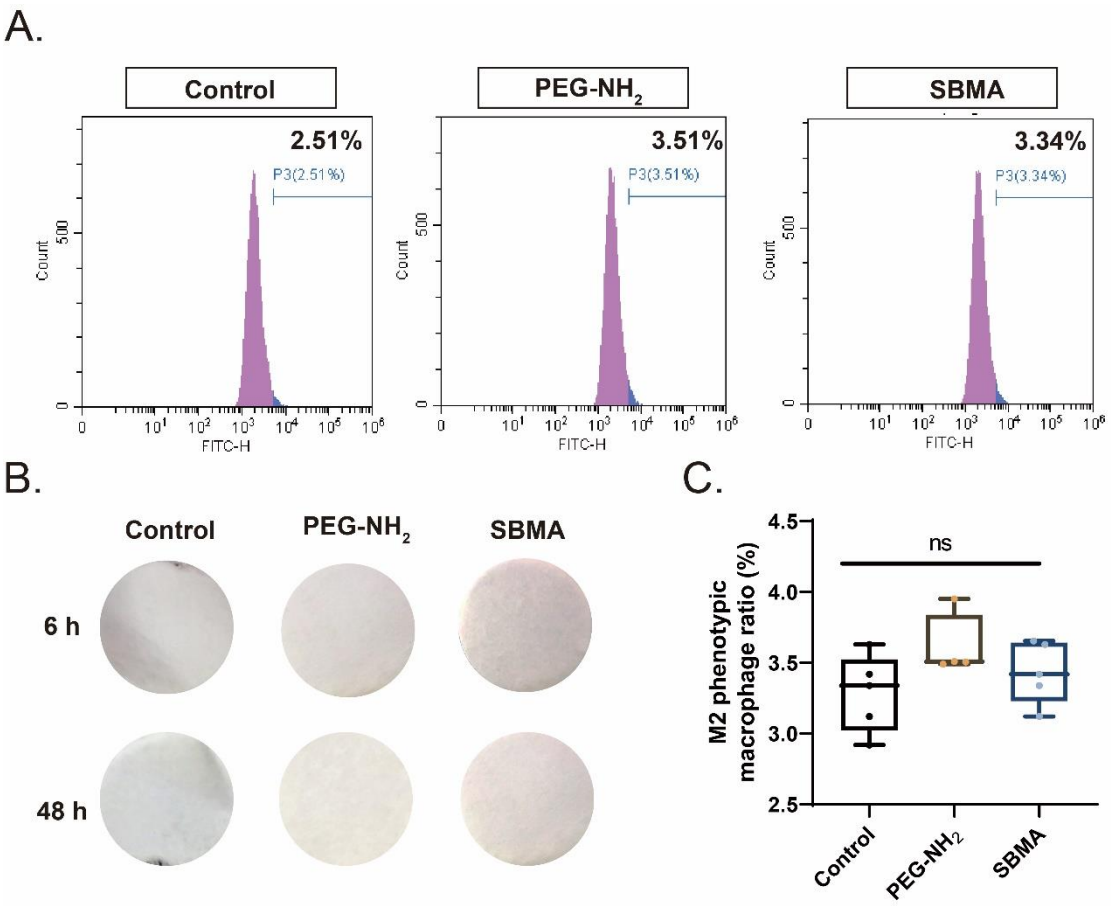

Supplementary Figure. 6 Evaluation of immunomodulatory capacity of PEG-NH2 and SBMA. A) Flow cytometry was used to analyze the effects of PEG-NH_2 and SBMA on the phenotype of macrophages. B) H_2S release of PEG-NH_2 and SBMA was investigated by lead acetate test paper method. Black is positively correlated with H_2S. Neither PEG-NH_2 nor SBMA demonstrated H_2S release capacity. C) Statistics of the proportion of CD206 positive cells (n=5). Data were expressed as mean ± SD, *P < 0.05, **P < 0.01, ***P < 0.001, and ****P < 0.0001. n means the number of independent experiments. For box plots, the lower edge denotes the first quartile (Q1, or the 25th percentile) of the data, the central line within the box signifies the median (Q2, or the 50th percentile), while the upper edge of the box corresponds to the third quartile (Q3, or the 75th percentile). The lower whisker extends to the minimum value, indicating its range of variation, and the upper whisker reaches the maximum value, demonstrating its variability. One-way ANOVA was used for analyzing the data.

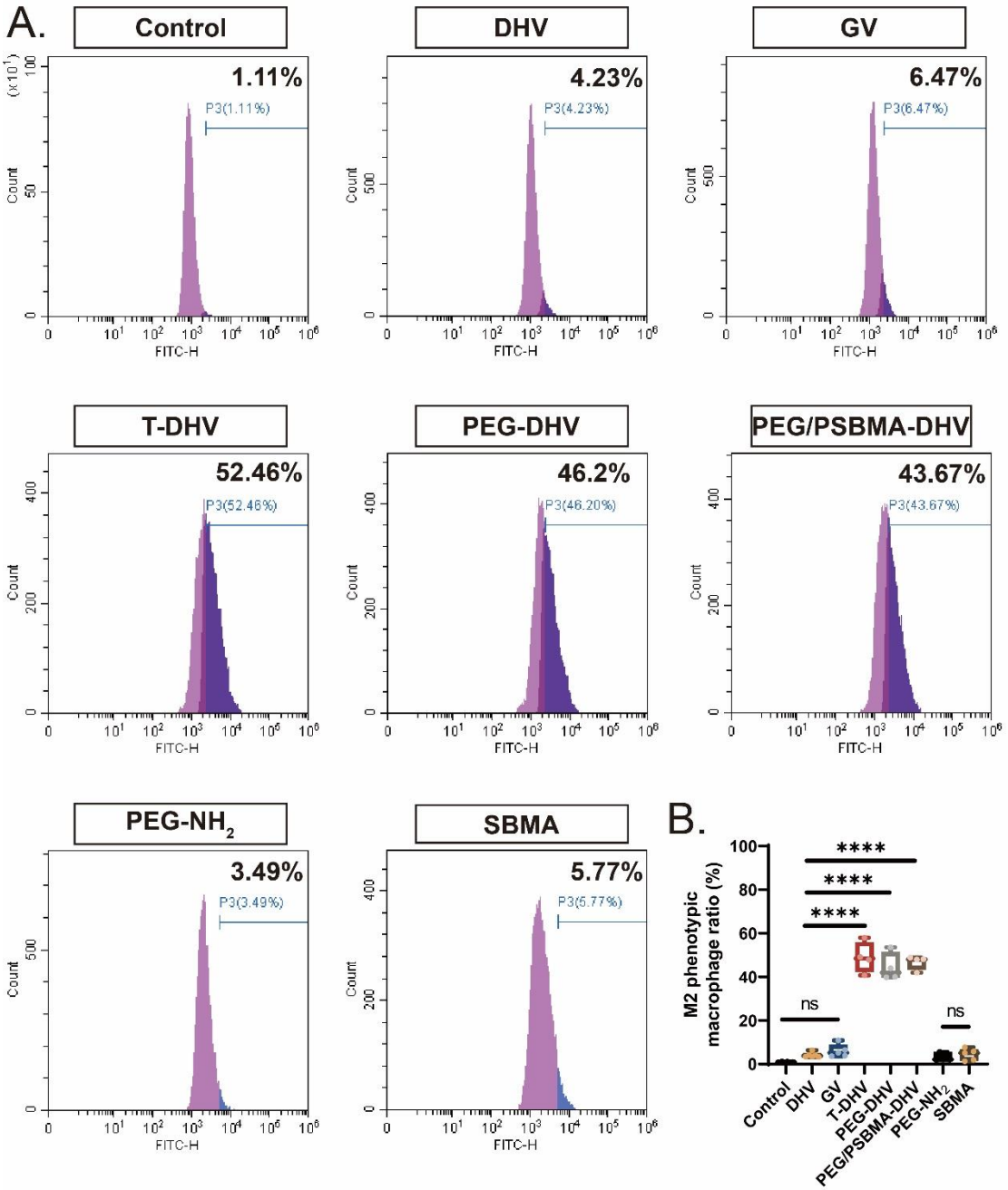

Supplementary Figure. 7 Evaluation of immunomodulatory capacity of PEG-NH2, SBMA, DHV, GV, T-DHV, PEG-DHV and PEG/PSBMA-DHV in the presence of cysteine. A) Flow cytometry was used to analyze the effects of PEG-NH_2, SBMA, DHV, GV, T-DHV, PEG-DHV and PEG/PSBMA-DHV on the phenotype of macrophages in the presence of cysteine. B) Statistics of the proportion of CD206 positive cells (n=5). Data were expressed as mean ± SD, *P < 0.05, **P < 0.01, ***P < 0.001, and ****P < 0.0001. n means the number of independent experiments. For box plots, the lower edge denotes the first quartile (Q1, or the 25th percentile) of the data, the central line within the box signifies the median (Q2, or the 50th percentile),

while the upper edge of the box corresponds to the third quartile (Q3, or the 75th percentile). The lower whisker extends to the minimum value, indicating its range of variation, and the upper whisker reaches the maximum value, demonstrating its variability. One-way ANOVA was used for analyzing the data.

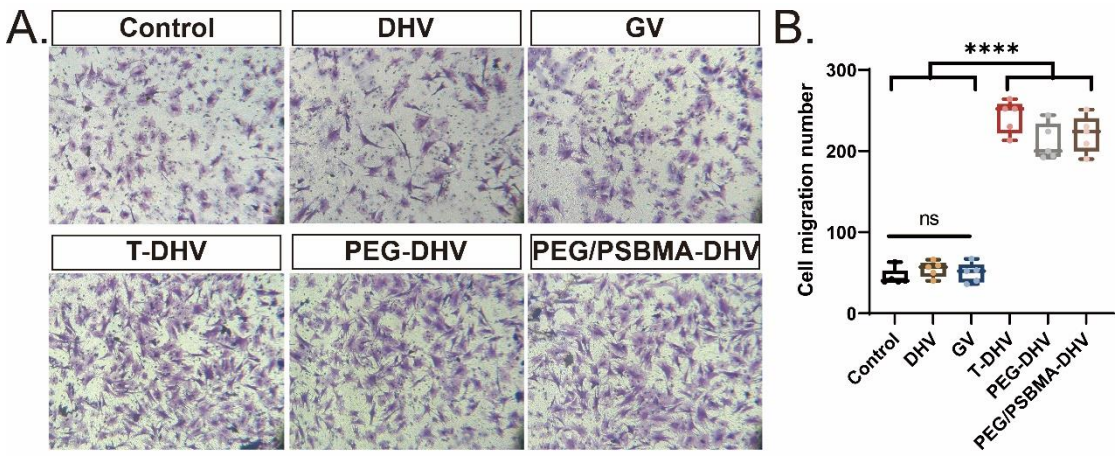

Supplementary Figure. 8 Cell invasion assay by transwell method was used to analyze the effect of macrophages on stem cell migration after T-DHV, PEG-DHV and PEG/PSBMA-DHV treatment. A) Bright field photos of the adherent cells on the lower surface of the upper chamber of transwell treated with different media conditions (n=5). B) Statistical analysis of the number of adherent cells (n=5). Data were expressed as mean ± SD, *P < 0.05, **P < 0.01, ***P < 0.001, and ****P < 0.0001. n means the number of independent experiments. For box plots, the lower edge denotes the first quartile (Q1, or the 25th percentile) of the data, the central line within the box signifies the median (Q2, or the 50th percentile), while the upper edge of the box corresponds to the third quartile (Q3, or the 75th percentile). The lower whisker extends to the minimum value, indicating its range of variation, and the upper whisker reaches the maximum value, demonstrating its variability. One-way ANOVA was used for analyzing the data.

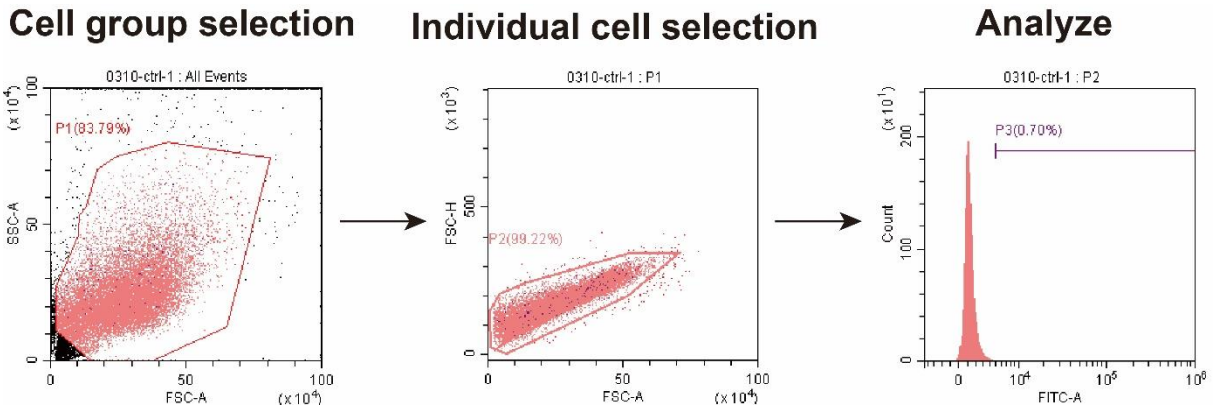

Supplementary Figure. 9 The gating strategy of flow cytometry.

Supplementary Table. 1 Cross-linking methods of heart valves

Crosslinking method	**Crosslinking agents**	**Ultimate tensile strength (MPa)**	**Degradability of crosslinking agent**	**Functionality**	**Toxicity**	**Crosslinking stability (Weight loss after collagenase treatment for 24 h)**	**Limitation**
1,1'-thiocarbonyldiimidazole	1,1'-thiocarbonyldiimidazole	11.79 ± 0.48	Yes	H_2S release, immune regulation, accelerated tissue regeneration	No	0.65 ± 2.29 %	
Glutaraldehyde	Glutaraldehyde[4,5]	10.87 ± 1.03	NO	No special	Cytotoxicity	4.5 - 6.44 %	Cytotoxicity，calcification，inflammation[5,6]
Natural products	Genipin[7]	14.26 ± 2.43	Yes	No special	No	81.58%	Exorbitant price, complex extraction process
	Procyanidins[8-10]			Antioxidant, reduce calcification, anti-calcification	No	14 - 40.85 %	Poor crosslinking stability[11]
	Curcumin[12,13]			Reduce calcification	No	76.2 - 88.84 %	Poor crosslinking stability[11]
EDC/NHS	EDC/NHS[14,15]	11.95 ± 1.48	NO	No special	No	3.74 - 4.51 %	NO
Epoxy compounds	Epoxy modified chitosan[16]	7.81	NO	No special	Cytotoxicity	6%	Cytotoxicity, calcification, inflammation[17]
Photo-crosslinking	Riboflavin[18]/ultraviolet light , Rose-bengal/visible light,[19] I2959	13.5 ± 1.5	NO	No special	Cytotoxicity	2.3 - 10 %	Low crosslinking efficiency,[11] cytotoxicity
Oxazolidines	Bicyclic hydromethyloxazolidine[20]	16.2 ± 3.2	NO	No special	No	7.06%	Complex synthesis
Polyphenol crosslinkers	3,4-Dihydroxybenzaldehyde,[21] Tannic acid[22,23]	13.5 ± 1.6	NO	No special	No	6.41%	Poor crosslinking stability[11]
Free radical polymerization	Acrylamide, [24,25]SBMA[5]	12.7 ± 1.7	NO	No special	Cytotoxicity	3.56 - 4 %	Cytotoxicity

Supplementary Table. 2 The primer sequences used in this paper

Name	Forward	Reverse
IL-10	GCTCTTACTGACTGGCATGAG	CGCAGCTCTAGGAGCATGTG
Arg1	TGGCTTGCGAGACGTAGAC	GCTCAGGTGAATCGGCCTTT

Supplementary References

1 Hine, C. et al. Endogenous Hydrogen Sulfide Production Is Essential for Dietary Restriction Benefits. *Cell* **160**, 132-144 (2015).

2 Liang, C.-C., Park, A. Y. & Guan, J.-L. In vitro scratch assay: a convenient and inexpensive method for analysis of cell migration in vitro. *Nat. Protoc.* **2**, 329-333 (2007).

3 Jin, S. et al. Conditioned medium derived from FGF-2-modified GMSCs enhances migration and angiogenesis of human umbilical vein endothelial cells. *Stem Cell Res. Ther.* **11,** 1-12 (2020).

4 Zhou, Y. et al. Nitric Oxide Generation and Endothelial Progenitor Cells Recruitment for Improving Hemocompatibility and Accelerating Endothelialization of Tissue Engineering Heart Valve. *Adv. Funct. Mater.* **33**, 2211267 (2022).

5 Yang, F. et al. Polyzwitterion-crosslinked hybrid tissue with antithrombogenicity, endothelialization, anticalcification properties. *Chem. Eng. J.* **410**, 128244 (2021).

6 Cheng, S. et al. Double‐Network Hydrogel Armored Decellularized Porcine Pericardium as Durable Bioprosthetic Heart Valves. *Adv. Healthcare Mater.* **11**, 2102059 (2022).

7 Lim, H. G., Kim, S. H., Choi, S. Y. & Kim, Y. J. Anticalcification effects of decellularization, solvent, and detoxification treatment for genipin and glutaraldehyde fixation of bovine pericardium. *EUR J CARDIO-THORAC* **41**, 383-390, 016 (2011).

8 Wang, X., Ma, B. & Chang, J. Preparation of decellularized vascular matrix by co-crosslinking of procyanidins and glutaraldehyde. *Bio-Med. Mater. Eng.* **26**, 19-30 (2015).

9 Zhai, W. et al. Crosslinking of decellularized porcine heart valve matrix by procyanidins. *Biomaterials* **27**, 3684-3690, (2006).

10 Yi, D., Wei, X., Sun, G., Liu, W. & Liu, Y. Calcification Resistance of Procyanidin-Treated Decellularized Porcine Aortic Valves In Vivo. *The Heart Surgery Forum* **12**, 24-29 (2009).

11 Zheng, C., Yang, L. & Wang, Y. Recent progress in functional modification and crosslinking of bioprosthetic heart valves. *Regener. Biomater.* **11**, rbad098 (2024).

12 Liu, J. et al. Curcumin-crosslinked acellular bovine pericardium for the application of calcification inhibition heart valves. *Biomed. Mater.* **15**, 045002 (2020).

13 Li, Y. et al. Therapeutic effects of EGF-modified curcumin/chitosan nano-spray on wound healing. *Regener. Biomater.* **8**, rbab009 (2021).

14 Luo, Y., Huang, S. & Ma, L. A novel detergent-based decellularization combined with carbodiimide crosslinking for improving anti-calcification of bioprosthetic heart valve. *Biomed. Mater.* **16**, 045022 (2021).

15 Lei, Y. et al. Bioprosthetic heart valves' structural integrity improvement through exogenous amino donor treatments. *J. Mater. Res.* **33**, 2576-2585 (2018).

16 Sun, Z. et al. Epoxy Chitosan-Crosslinked Acellular Bovine Pericardium with Improved Anti-calcification and Biological Properties. *ACS Appl. Bio Mater.* **3**, 2275-2283 (2020).

17 Ma, B., Wang, X., Wu, C. & Chang, J. Crosslinking strategies for preparation of extracellular matrix-derived cardiovascular scaffolds. *Regener. Biomater.* **1**, 81-89 (2014).

18 Lei, Y., Guo, G., Jin, W., Liu, M. & Wang, Y. Riboflavin photo‐cross‐linking method for improving elastin stability and reducing calcification in bioprosthetic heart valves. *Xenotransplantation* **26**, 12481 (2019).

19 Yang, F., Xu, L., Guo, G. & Wang, Y. Visible light‐induced cross‐linking of porcine pericardium for the improvement of endothelialization, anti‐tearing, and anticalcification properties. *J. Biomed. Mater. Res., Part A* **110**, 31-42, 37263 (2021).

20 Chen, X. et al. Functional non-glutaraldehyde treated porcine pericardium for anti-coagulation, anti-calcification, and endothelial proliferation bioprosthetic heart valves. *J. Leather Sci. Eng.* **4**, 1-13 (2022).

21 Wu, B. et al. Cross-Linking Porcine Pericardium by 3,4-Dihydroxybenzaldehyde: A Novel Method to Improve the Biocompatibility of Bioprosthetic Valve. *Biomacromolecules* **22**, 823-836, 0c01554 (2020).

22 Dąbrowska, K. Z., Turek, A., Grzejda, R. & Kobielarz, M. Mechanical properties of the porcine pericardium extracellular matrix cross-linked with glutaraldehyde and tannic acid. *Acta. Bioeng. Biomech.* **24**, 21-31 (2022).

23 Liu, Y. et al. The hybrid crosslinking method improved the stability and anti-calcification properties of the bioprosthetic heart valves. *Front. Bioeng. Biotechnol.* **10**, 1008664 (2022).

24 Guo, G. et al. Radical polymerization-crosslinking method for improving extracellular matrix stability in bioprosthetic heart valves with reduced potential for calcification and inflammatory response. *Acta Biomater.* **82**, 44-55, (2018).

25 Guo, G. et al. A method for simultaneously crosslinking and functionalizing extracellular matrix-based biomaterials as bioprosthetic heart valves with enhanced endothelialization and reduced inflammation. *Acta Biomater.* **119**, 89-100, (2021).